Journal of Applied Physics

Direct measurements of the magnetocaloric effect of $Fe_{49}Rh_{51}$ using the mirage effect

Cite as: J. Appl. Phys. **127**, 233905 (2020); https://doi.org/10.1063/5.0006355
Submitted: 03 March 2020 . Accepted: 31 May 2020 . Published Online: 17 June 2020

A. A. Amirov, F. Cugini, A. P. Kamantsev, T. Gottschall, M. Solzi, A. M. Aliev, Yu. I. Spichkin, V. V. Koledov, and V. G. Shavrov

Journal of Applied Physics ARTICLE scitation.org/journal/jap

Direct measurements of the magnetocaloric effect of $Fe_{49}Rh_{51}$ using the mirage effect

Cite as: J. Appl. Phys. **127**, 233905 (2020); doi: 10.1063/5.0006355
Submitted: 3 March 2020 · Accepted: 31 May 2020 ·
Published Online: 17 June 2020

A. A. Amirov,[1,2,a)] F. Cugini,[3] A. P. Kamantsev,[1,4] T. Gottschall,[5] M. Solzi,[3] A. M. Aliev,[1,2] Yu. I. Spichkin,[6] V. V. Koledov,[4] and V. G. Shavrov[4]

AFFILIATIONS

[1]Laboratory of Novel Magnetic Materials, Institute of Physics, Mathematics and Information Technology, Immanuel Kant Baltic Federal University, Kaliningrad 236013, Russia
[2]Amirkhanov Institute of Physics of Dagestan Federal Research Center, Russian Academy of Sciences, Makhachkala 367003, Russia
[3]Department of Mathematical, Physical and Computer Sciences, University of Parma, Parco Area delle Scienze 7/A, 43124 Parma, Italy
[4]Kotelnikov Institute of Radio Engineering and Electronics, Russian Academy of Sciences, 11/7 Mokhovaya Str., 125009 Moscow, Russia
[5]Dresden High Magnetic Field Laboratory (HLD-EMFL), Helmholtz-Zentrum Dresden-Rossendorf, D-01328 Dresden, Germany
[6]Advanced Magnetic Technologies and Consulting LLC, 142190, Promyshlennaya 4, Troitsk, Russia

Note: This paper is part of the Special Topic on: Multicalorics.
[a)]**Author to whom correspondence should be addressed:** amiroff_a@mail.ru

ABSTRACT

The magnetocaloric effect in the $Fe_{49}Rh_{51}$ alloy was systematically studied using three different approaches: in-field differential scanning calorimetry, standard direct measurement of the adiabatic temperature change, and a non-contact method based on a thermo-optical phenomenon, the mirage effect, which was able to directly test the magnetocaloric response induced by a fast magnetic field variation. The metamagnetic phase transition of $Fe_{49}Rh_{51}$ was studied in the temperature range of 290–330 K at magnetic fields up to 1.8 T through magnetic and calorimetric measurements. The estimated parameters of phase transition were comparable with the literature data. The values of adiabatic temperature change obtained with the three methods (calorimetry, standard direct measurement, and mirage-based technique), which explore three different time scales of the field variation (static field, 1 T s^{-1}, 770 T s^{-1}), were consistent, proving the absence of dynamic constraints in the first-order magnetostructural transition at the maximum field sweep rate.

I. INTRODUCTION

Materials with a first-order magnetic phase transition (FOMPT) are intensively investigated, not only for the basic research interest related to the strong interplay between their magnetic, electronic, and structural subsystems, but also because of their potential application in efficient energy conversion devices and spintronics technologies.[1–3] One of the most interesting results of these interactions is the so-called "giant" magnetocaloric effect (MCE), which consists in an adiabatic temperature (ΔT_{AD}) or an isothermal entropy change (ΔS_T) of a material caused by a magnetic field variation.[4] However, despite the large MCE values that have been observed, there are several disadvantages of FOMPT materials that limit their usability.[3,5] One of the main problems is related to the presence of hysteresis, which limits the reversible MCE that can be exploited in cyclic magnetic fields.[6–9] For an active magnetic regenerator of a magnetocaloric (MC) cooling system, the operation frequency should be as high as possible to work efficiently. This means that it is important to study the dependence of the MCE of different materials not only on the magnetic field change but also on the magnetic field sweep rate. Interesting results were reported by Gottschall *et al.*[10] for a Ni–Mn-based Heusler alloy, where the direct MCE was studied under different field sweep rates

from 0.01 up to 1500 T s^{-1}. It was demonstrated that the MCE depends on the sweep rate of the magnetic field, and dynamic effects of the first-order phase transition could limit the application of the material in cooling devices working at high frequencies. It should be noted that most of the experimental works report magnetocaloric properties measured with magnetic field changes up to 2 T and frequencies less than 1 Hz.[2,11,12] From this point of view, it is of great importance to measure the MCE in similar magnetic field variations (obtainable typically with a Halbach-type permanent magnet), but with faster sweep rates in order to study the dynamical effects of FOMPT materials.[13]

Another issue that should be considered is related to the shape of the MCE material (powder, ribbon, film, wire, and), because typically very fine structures are used in magnetocaloric heat exchangers.[3,14] However, direct methods do not provide precise measurements if the thermocouple mass is comparable with the mass of the sample or in the case of a bad thermal contact.[15] Different approaches were used in order to limit these experimental issues, such as the design of special low-mass micro-thermocouples[16,17] or the sputtering of thermometer on the top of sample surface.[18] In parallel, several non-contact methods based on lock-in thermography using an IR camera,[19] a non-contact thermopile,[20] a HgCdTe-infrared detector with lock-in systems,[21] and special infrared optical fiber temperature sensors[22] were developed for direct magnetocaloric measurements. Recently, Cugini *et al.*[23,24] proposed a novel method based on the thermo-optical mirage effect using pulsed magnetic fields, which is suitable for the determination of the magnetocaloric properties of micro-scale thin objects.

The aim of this work is the direct measurement of the MCE of a FeRh alloy, as a model FOMPT material with outstanding adiabatic temperature changes,[25] by means of standard methods (in-field differential scanning calorimetry and the direct measurement of adiabatic temperature change with a thermocouple) and the new approach based on the mirage effect, which combines a non-contact measurement technique with a pulsed magnetic field. These three different methods allow us to test the magnetocaloric response of FeRh at three different time scales of the field variation (static field, 1 T s^{-1}, and 770 T s^{-1}), with the aim to investigate the possible kinetic effects associated with the first-order magnetostructural transition.

II. MATERIALS AND METHODS

The chemical composition corresponding to $Fe_{49}Rh_{51}$ and the microstructure of the sample was examined by a scanning electron microscope (JSM-6390LV) integrated with an energy dispersive x-ray spectroscopy (EDX) analyzer (Oxford X-Acta). XRD analysis confirmed that sample has a *B2* chemically ordered CsCl-type structure with the small presence of a disordered *fcc* γ phase. Calculated from XRD data, the lattice parameters *a* for *B2* and γ phases were 2.991 and 3.768, respectively. The estimation of volume ratio of phases showed that the concentration of the *fcc* γ phase is about 7.4% (details can be found in Ref. 26). The magnetic behavior of the alloy as a function of temperature in different magnetic fields was obtained using a physical property measurement system (PPMS). Preliminary studies of the magnetostructural transition were performed by means of a differential scanning calorimeter (DSC) based on thermoelectric modules, which works in a magnetic field up to 1.8 T.[27] Specific heat was measured with temperature sweeps on heating and on cooling at a constant sweep rate (2 K min^{-1}) between 250 K and 380 K, in zero applied magnetic field, 1 T, and 1.8 T.

The direct MCE experiments were carried out with an upgraded version of a commercial setup using a magnetic field source based on the dipole Halbach structure principle with field amplitude of 1.8 T and a maximum field change rate up to 6 T/s (AMT&C). The temperature of the sample was measured using a differential thermocouple (type T), fabricated by copper and constantan wires with a diameter of 25 μm. To improve the thermal contact, the thermocouple junction was flattened, connected by electrical welding, bonded with the sample surface using silver epoxy, and clamped with further drying at 70 °C for 12 h.

In direct measurements, the heat that is released due to the MCE is partially lost on the thermocouple and adhesive. In the case of samples with small dimensions, the mass of the thermocouple attached with adhesive is a key problem for precise measurements.[28,29] Thus, the observed value of MCE (the experimental adiabatic temperature change ΔT_{exp}) is usually smaller than the real temperature change of the sample (ΔT_{AD}) and depends on the ratio between the heat capacity of the sample and thermocouple with glue. This relation can be represented by the following equation:

$$\Delta T_{AD} = \Delta T_{exp}(1 + C_{thermocouple}/C_{sample}), \quad (1)$$

where C_{sample} and $C_{thermocouple}$ are the heat capacities of the sample and the thermocouple with glue, respectively.[30] As seen, the experimentally measured ΔT_{exp} approaches the real ΔT_{AD} value when $C_{thermocouple}/C_{sample}$ tends to 0. It means that magnetocaloric measurements are more accurate when the specific heat and mass of the thermocouple with glue are significantly smaller compared to those of the sample. Our calculations of the differences between the experimental and the real values of the adiabatic temperature changes based on the analysis of the heat capacity ratio $C_{thermocouple}/C_{sample}$ [Eq. (1)] show that the contribution of the $C_{thermocouple}$ to total capacity of the system (sample + thermocouple with glue) is less than 2%.

Conventional direct measurements were performed in a discontinuous protocol, as described in Figure 9(b) of Ref. 29: before each measurement, the sample was cooled down to 240 K to erase the memory of the material and then the sample was heated to the desired temperature and ΔT_{AD} was measured by applying a 1.8 T magnetic field with an overall sweeping rate of 1 T s^{-1}.

The adiabatic temperature change of the sample was measured also using an alternative non-contact method based on the thermo-optical "mirage effect," which consists in the deflection of a light beam by a thermal gradient.[23,24] This technique measures the change of the sample temperature, induced by a magnetic field pulse, by detecting the deflection of a laser beam grazing the sample surface. The beam is deflected by the thermal gradient that is formed in the thin air layer overlying the sample surface due to the temperature change of the sample. The angle of deflection of the laser beam is proportional to the temperature gradient and the length of the laser path across the temperature gradient, which corresponds to the sample length since each part of the sample experiences the same temperature change.[23,24] By measuring the deflection of the laser

beam and by calibrating the setup with a reference material (gadolinium), it is possible to obtain the absolute temperature change induced in the sample by the applied magnetic field. The pulsed magnetic field, that was used, has a maximum amplitude of 1 T, a rise time of about 1.3 ms and a maximum sweep rate of 1420 T s^{-1} (average sweep rate: 770 T s^{-1}). It was demonstrated that the thermal diffusion time to the gas layer next to the sample surface is fast enough to probe the magnetocaloric response of the material to short pulses of the order of milliseconds.[23] The fast response time and the limited heat capacity of the gas layer ensure that we can consider the change in temperature to be adiabatic. A standard Pt100 temperature sensor is placed inside the sample holder in order to measure the absolute temperature of the sample before to apply the magnetic field and perform the magnetocaloric (MC) measurement.

III. RESULTS AND DISCUSSION

Figure 1 shows the temperature dependences of the magnetization of the $Fe_{49}Rh_{51}$ sample in different magnetic fields: 0.1 (a), 1, and 1.8 T (b). In all M(T) curves, the metamagnetic phase transition from the antiferromagnetic (AFM) to the ferromagnetic (FM) phase is visible.

The magnetic field shifts the transition temperature to lower temperatures with a rate of about $dT_t/\mu_0 dH = -7.2$ K/T, which is close to the value (−8.5 K/T) for a similar $Fe_{49}Rh_{51}$ alloy reported by Chirkova *et al.*[7] For the estimation of the transition temperatures and the thermal hysteresis width, the M(T) curves in 0.1 T and their temperature derivative dM/dT were used [Fig. 1(a)]. Based on these results, the transition temperatures of the sample are $T_{AFM-FM} = 320.5$ K and $T_{FM-AFM} = 314$ K, resulting in a thermal hysteresis of about ∼6.5 K. It should be noted that these parameters as well as other magnetic characteristics strongly depend on the fabrication process and the subsequent heat treatment protocol (temperature, time, cooling rate).[7,8,25,34,35] As known, at room temperature $Fe_{1-x}Rh_x$ with $47\% \leq x \leq 52\%$ has two types of crystal structure: *B2* (or α'), a chemically ordered CsCl-type structure, and a disordered *fcc* γ phase.[31]

The AFM–FM transition of FeRh alloy occurs in the chemically ordered *B2* phase; the γ phase is not involved in this process. The protocol of heat treatment plays a key role in the formation of the ordered CsCl crystal structure, the coexistence between *B2* (or α') and the disordered *fcc* γ phase and the presence of internal stresses between them, which affect the magnetic properties and parameters of phase transition.[32] Moreover, for the correct estimation of the transition temperatures, measurements in zero or close to zero magnetic field are recommended. For this reason, specific heat measurements with and without magnetic field were carried out using the DSC technique for the analysis of the magnetothermal and magnetocaloric properties.

Figure 2 shows the DSC measurements in 0, 1, and 1.8 T applied magnetic field, obtained both on heating and on cooling.

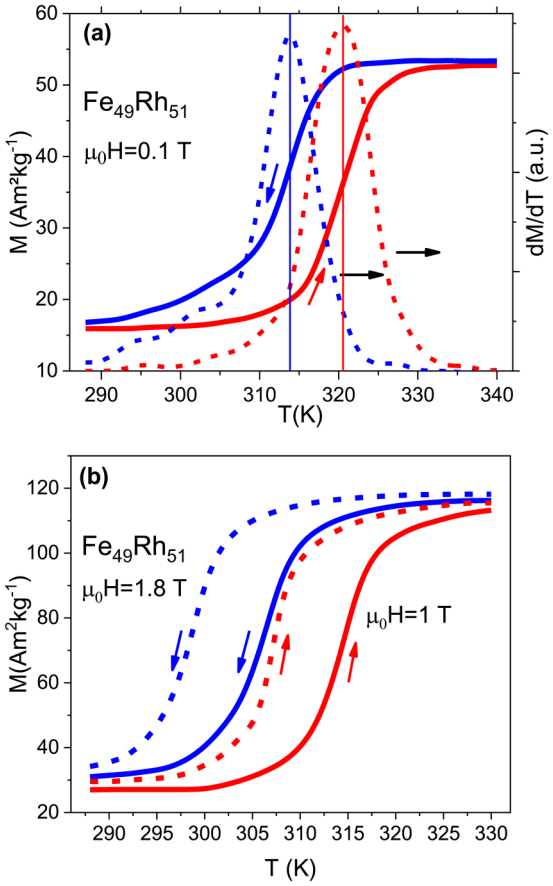

FIG. 1. Temperature dependences of magnetization for $Fe_{49}Rh_{51}$ measured in 0.1 (a), 1, and 1.8 T(b) magnetic fields. Right plot (a)—temperature dependence of dM/dT in 0.1 T magnetic field.

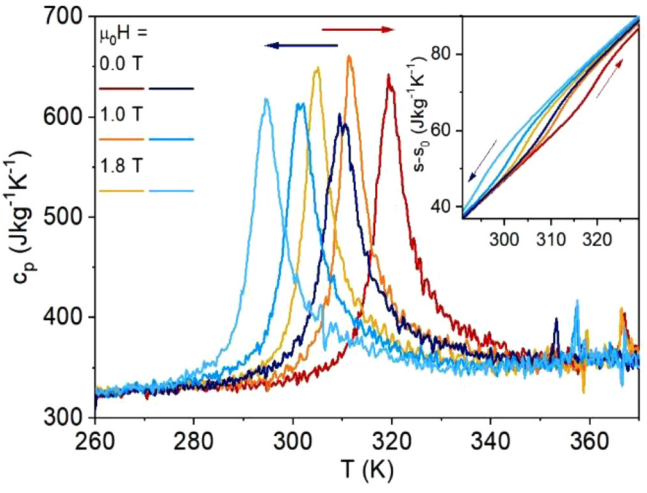

FIG. 2. $c_P(T,H)$ curves obtained from DSC measurements in 0, 1, and 1.8 T magnetic field on heating and cooling. Inset: corresponding entropy curves calculated from DSC data.

The peaks of the heat capacity are due to the first-order magneto-structural transition of the material. The transition on heating occurs at 319.8 K in zero applied field. The magnetic field shifts the transition temperature, by promoting the high temperature phase, with a rate $dT_t/\mu_0 dH = -8.3 \pm 0.4$ K/T, in agreement with Ref. 7 and slightly lower than the result reported in Ref. 35.

The transition is characterized by a thermal hysteresis of about 9 K, which is not significantly affected by the application of magnetic field. We can also appreciate the broadening of the transition, which is characterized by a width of about 16 K, a larger value compared to the DSC measurements reported in Refs. 7 and 35. The latent heat (λ) of the fully transformed transition was calculated by integrating the $c_p(T)$ peaks after subtraction of the baseline between the start and finish temperatures of the transformation.[33] We obtained a latent heat of 3010 ± 100 J kg^{-1}, showing a small increase due to the application of the magnetic field (+4% for a $\mu_0\Delta H$ of 1.8 T). From the latent heat, it is possible to estimate the entropy change corresponding to the fully induced phase transition $\Delta S_{full} \sim \lambda/T_c = 9.7 \pm 0.4$ J kg^{-1} K^{-1}. This value is slightly lower to the maximum entropy variation that can be calculated by using the Clausius–Clapeyron equation from magnetometry data $\Delta S_T \sim 11$ J kg^{-1} K^{-1}.

By integrating the DSC measurements and comparing the data obtained in different applied fields, both the isothermal entropy change and the adiabatic temperature change were derived.[27] The entropy change was calculated by subtracting the $S(T)$ entropy curve at zero field from the one at $\mu_0 H = 1$ or 1.8 T (inset of Fig. 2),

$$\Delta S_T(T, \mu_0 H) = \int_{T_0}^{T} \frac{C_p(T, H) - C_p(T, 0)}{T} dT + \Delta S_T(T_0, \mu_0 H), \quad (2)$$

where T_0 is the starting temperature of measurement, in the region far below the transformation. We neglected the correction due to the in-field magnetic entropy variation at T_0 [$\Delta S_T(T_0, \mu_0 \Delta H)$].[27] Likewise, the adiabatic temperature change was calculated by subtracting the inverted $S(T,H)$ curves. The error due to the numerical manipulation of specific heat data, reported in Fig. 3, was estimated following the discussion of Ref. 27.

Figure 3 shows the isothermal entropy change $|\Delta S_T(T)|$ and the adiabatic temperature change $|\Delta T_{AD}(T)|$ for a magnetic field variation of 1 T and 1.8 T derived from measurements on heating and cooling. The shift in temperature between the $\Delta S_T(T)$ and $\Delta T_{ad}(T)$ peaks obtained from measurements on cooling and on heating highlights the effect of thermal hysteresis, characteristic of first-order transitions. The maximum $|\Delta S_T|$ and $|\Delta T_{AD}|$ values for a $\mu_0\Delta H = 1.8$ T are lower than the results reported in Refs. 7, 34, and 35. This is probably due to the broadening of the transition, as discussed in Ref. 33. The maximum value of entropy change (8.0 ± 0.3 J kg^{-1} K^{-1}), induced by 1.8 T field change, is lower than the entropy change calculated for a fully induced phase from the latent heat (9.7 ± 0.4 J kg^{-1} K^{-1}) and by using the Clausius–Clapeyron equation (11 J kg^{-1} K^{-1}). This means that even the 1.8 T magnetic field change is not enough to induce the full transformation, because of the broadening of the transition.[33]

The measurement of the adiabatic temperature change collected by the setup based on the mirage effect is illustrated for different starting temperatures in Fig. 4 together with the time profile of the pulsed magnetic field. Considering the hysteretic

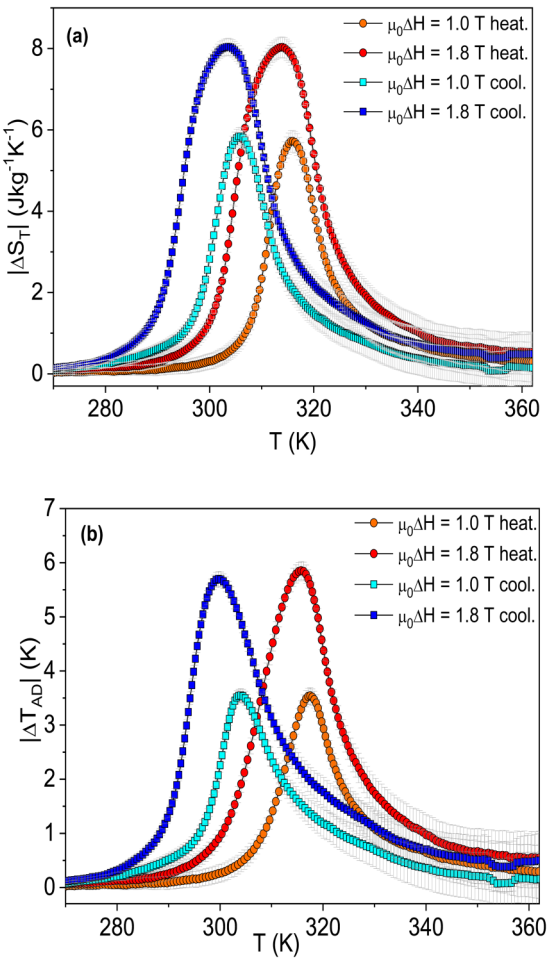

FIG. 3. Isothermal entropy $|\Delta S_T|$ (a) and adiabatic temperature changes $|\Delta T_{AD}|$ (b) derived from DSC data performed on heating and cooling for different magnetic field variations (1 T and 1.8 T).

character of the transition, a phase-reset protocol for an inverse magnetocaloric material was used, in order to obtain the maximum effect exploitable with a 1 T magnetic field variation. The protocol is schematized in Figure 9(b) of Ref. 29 with the green arrows. Before each measurement, the sample was cooled down to 280 K in order to stabilize the low-temperature AFM phase. Then, the sample was heated to the desired temperature with a controlled sweep rate of 1 K/min, avoiding temperature overshoots and time delays.

After reaching the temperature set point, the adiabatic temperature change was measured by applying the magnetic field pulse [$\mu_0 H_{max} = 1$ T, Fig. 4(a)]. Between 314 and 324 K, we can observe a decrease of the sample temperature due to the AFM to FM transition caused by the application of the magnetic field [Fig. 4(b)]. When the magnetic field decreases, only a very small reversible effect is induced in the sample due to the large thermal hysteresis. The wavy pattern of the $T(t)$ measured with the mirage effect is not

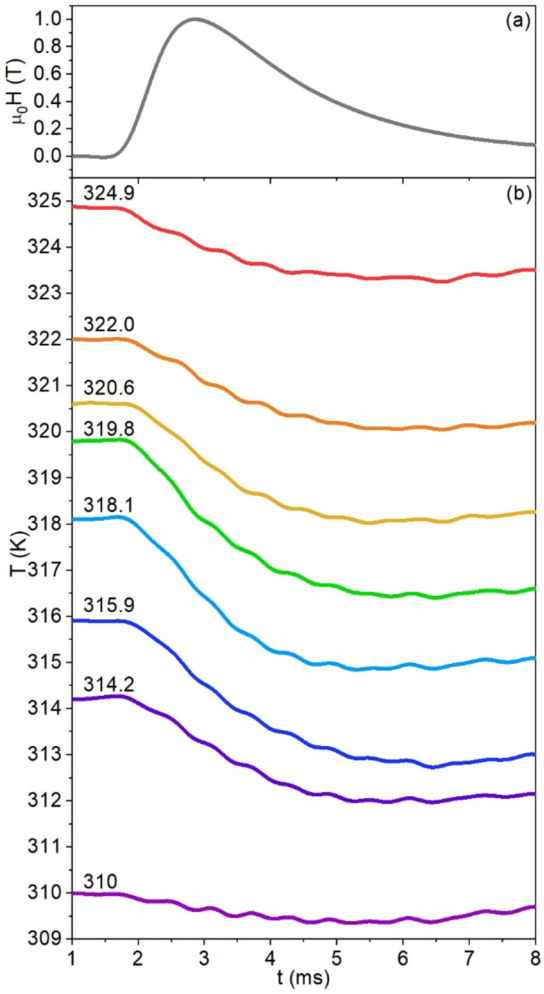

FIG. 4. Time dependence of the magnetic field pulse (a) and temperature change of sample at different starting temperatures measured by the mirage-based setup (b).

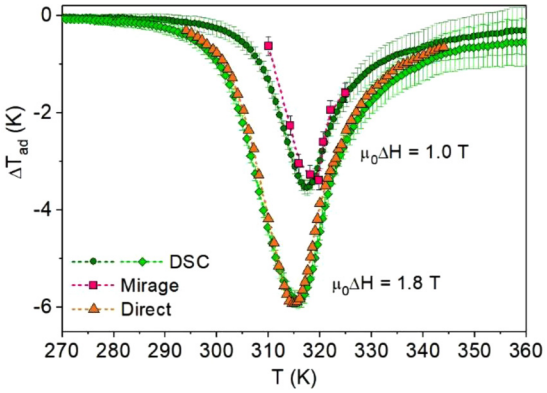

FIG. 5. Adiabatic temperature change ΔT_{AD} of $Fe_{49}Rh_{51}$ as a function of temperature in 1 T and 1.8 T magnetic field change, measured by three different methods (DSC, mirage effect, and standard direct technique).

related to the MCE of the sample, but it is due to residual vibrations that perturb the optical system of measurement.

Figure 5 presents the adiabatic temperature change ΔT_{AD} data that were collected through the three methods. $\Delta T_{AD}(T)$ directly measured through the standard direct technique (orange triangles) and the mirage-based setup (purple squares) resulted consistent with the values derived from DSC data (green circles and diamonds). The small temperature shift (<1 K) between the curves at $\mu_0\Delta H = 1$ T is due to an experimental systematic error in the measurement of the sample starting temperature in the mirage-based setup. Indeed, the measurement of the sample temperature is obtained, before performing the MC measurement, by a standard resistive sensor placed inside the sample holder. When the sample temperature is varied in order to reach the starting temperature for the MC measurement, a temperature gradient arises between the sample and the sensor, which cannot be avoided due to the necessity to prevent temperature overshoots and long time delays, because of the hysteretic character of the transition.

Considering the maximum of the $\Delta T_{AD}(T)$ curves, we obtained -3.4 ± 0.2 K (mirage-based setup) and -3.50 ± 0.15 K (DSC) for $\mu_0\Delta H = 1$ T; and -5.9 ± 0.1 K (standard direct method) and -5.85 ± 0.17 K (DSC) for $\mu_0\Delta H = 1.8$ T. Both pairs of data are consistent considering the experimental errors. The result at $\mu_0\Delta H = 1$ T is in the middle between the value reported for a $Fe_{50.4}Rh_{49.6}$ sample in Ref. 8 ($\Delta T_{AD} \sim 3$ K) and that ($\Delta T_{AD} \sim 4$ K) reported for $Fe_{49}Rh_{51}$ in Ref. 7. This difference can be related to the small variation of chemical composition, to a different effect of the post-synthesis heat treatment, or to the presence of inhomogeneities that can modify the transition temperature and the broadening of the transformation with significant effect on the MCE.[8,33]

Returning to the results of this work, it is important to underline the agreement between ΔT_{AD} data obtained by the three different methods, which explore very different time scales of the field variation. With the DSC, the measurements are performed under a static magnetic field and the transition is induced by a temperature change. DSC data result in a "static" entropy vs temperature diagram. ΔT_{AD} calculated from these data does not consider a time variation of the magnetic field. This means that it should correspond to ΔT_{AD} measured with a very slow field variation, provided that the adiabatic condition is preserved. Instead, the direct measurements probe the dynamic response of the transition to the field variation. The two utilized experimental setups are characterized by very different field sweep rates. The standard direct method works in the time scale of seconds with an average sweep rate of the field of 1 T s^{-1}. Instead, the mirage-based setup exploits a field change in the time scale of milliseconds, with an average sweep rate of 770 T s^{-1}. The agreement between both the direct ΔT_{AD} measurements (standard and mirage-based technique) and the values calculated from iso-field DSC data demonstrates the absence of kinetic constraints that hinder the magneto-structural transition of the sample on a time scale down to milliseconds. This result, obtained

by measuring the caloric effect associated with the magneto-structural transition, agrees with the conclusions on the structural and magnetic dynamics of the phase transition of a FeRh film reported in Ref. 36. The authors studied the dynamics of the magneto-structural transition of FeRh by the combination of time-resolved x-ray diffraction and the magneto-optical Kerr effect. They concluded that the transformation, induced by a laser pulse, is composed by two processes: the nucleation of independent ferromagnetic domains and the growth of the ferromagnetic domains aligned to the applied magnetic field. Both the processes occur in the picosecond time scale and the only limit of the transition dynamic is set by the speed of sound. Our results demonstrate that the caloric response follows the magneto-structural transition, at least down to the millisecond time scale. This means that the FeRh material can be hypothetically utilized in a MC device that exploits a field variation at a frequency up to about 800 Hz without a worsening of its MC response after engineering the large thermal hysteresis.

IV. CONCLUSION

In this research, the adiabatic temperature change induced by a magnetic field change in the vicinity of the order–order FOMPT of a $Fe_{49}Rh_{51}$ sample was measured by three different methods: (1) a standard direct method that exploits a thermocouple placed on the sample and a field variation of 1.8 T in about 1.8 s; (2) a non-contact direct method based on the thermo-optical mirage effect that measures the temperature variation induced in the sample by a pulsed magnetic field of 1 T amplitude and an average sweep rate of 770 T s^{-1}; and (3) the indirect method using in-temperature DSC data acquired in different applied magnetic fields (0 T, 1 T, and 1.8 T). All the obtained ΔT_{AD} data resulted in good agreement. This confirms the absence of kinetic constraints in the magnetostructural transformation induced on the millisecond time scale and that the caloric response, on this time scale, follows the magnetostructural transition. Moreover, this paper proves, for the first time, the possibility to use the mirage-based setup to test the magnetocaloric response induced by a pulsed magnetic field also in materials showing an inverse MCE, thus opening new opportunities to test the dynamic response of magnetocaloric materials at high frequencies.

ACKNOWLEDGMENTS

The work was partially supported by the Helmholtz Association via the Helmholtz-RSF Joint Research Group (Project No. HRSF-0045) and the HLD at HZDR, a member of the European Magnetic Field Laboratory (EMFL). A.A.A. acknowledges the Russian Science Foundation for support in magnetocaloric measurements (Grant No. 18-79-10176). A.M.A. acknowledges the 5 top 100 Russian Academic Excellence Project at the Immanuel Kant Baltic Federal University. The authors are grateful to Professor A. Tishin (Faculty of Physics, M.V. Lomonosov Moscow State University) for useful notes and discussions.

DATA AVAILABILITY

The data that support the findings of this study are available from the corresponding author upon reasonable request.

REFERENCES

[1]D. Sander *et al.*, J. Phys. D: Appl. Phys. **50**, 363001 (2017).
[2]V. Franco, J. S. Blázquez, J. J. Ipus, J. Y. Law, L. M. Moreno-Ramírez, and A. Conde, Prog. Mater. Sci. **93**, 112 (2018).
[3]T. Gottschall, D. Benke, M. Fries, A. Taubel, I. A. Radulov, K. P. Skokov, and O. Gutfleisch, Adv. Funct. Mater. **27**, 1606735 (2017).
[4]V. K. Pecharsky and K. A. Gschneidner, Jr., Phys. Rev. Lett. **78**, 4494 (1997).
[5]A. M. Tishin, J. Magn. Magn. Mater. **316**, 351 (2007).
[6]A. M. Aliev, A. B. Batdalov, L. N. Khanov, A. P. Kamantsev, V. V. Koledov, A. V. Mashirov, V. G. Shavrov, R. M. Grechishkin, A. R. Kaul', and V. Sampath, Appl. Phys. Lett. **109**, 202407 (2016).
[7]A. Chirkova, K. P. Skokov, L. Schultz, N. V. Baranov, O. Gutfleisch, and T. G. Woodcock, Acta Mater. **106**, 15 (2016).
[8]V. I. Zverev, A. M. Saletsky, R. R. Gimaev, A. M. Tishin, T. Miyanaga, and J. B. Staunton, Appl. Phys. Lett. **108**, 192405 (2016).
[9]T. Gottschall, E. Stern-Taulats, L. Mañosa, A. Planes, K. P. Skokov, and O. Gutfleisch, Appl. Phys. Lett. **110**, 223904 (2017).
[10]T. Gottschall, K. P. Skokov, F. Scheibel, M. Acet, M. Ghorbani-Zavareh, Y. Skourski, J. Wosnitza, M. Farle, and O. Gutfleisch, Phys. Rev. Appl. **5**, 024013 (2016).
[11]T. Gottschall, K. P. Skokov, M. Fries, A. Taubel, I. Radulov, F. Scheibel, D. Benke, S. Riegg, and O. Gutfleisch, Adv. Energy Mater. **9**, 1901322 (2019).
[12]J. Lyubina, J. Phys. D Appl. Phys. **50**, 053002 (2017).
[13]A. P. Kamantsev, A. A. Amirov, Y. S. Koshkid'ko, C. Salazar Mejía, A. V. Mashirov, A. M. Aliev, V. V. Koledov, and V. G. Shavrov, Phys. Solid State **62**(1), 160 (2020).
[14]A. Kitanovski, Adv. Energy Mater. **10**, 1903741 (2020).
[15]T. Kihara, X. Xu, W. Ito, R. Kainuma, and M. Tokunaga, Phys. Rev. B **90**, 214409 (2014).
[16]T. Gottschall, M. D. Kuz'min, K. P. Skokov, Y. Skourski, M. Fries, O. Gutfleisch, M. Ghorbani Zavareh, D. L. Schlagel, Y. Mudryk, V. Pecharsky, and J. Wosnitza, Phys. Rev. B **99**, 134429 (2019).
[17]A. Aliev, A. Batdalov, L. Khanov, V. Koledov, V. Shavrov, I. Tereshina, and S. Taskaev, J. Alloys Compd. **676**, 601–605 (2016).
[18]T. Kihara, Y. Kohama, Y. Hashimoto, S. Katsumoto, and M. Tokunaga, Rev. Sci. Instrum. **84**, 074901 (2013).
[19]Y. Hirayama, R. Iguchi, X.-F. Miao, K. Hono, and K. Uchida, Appl. Phys. Lett. **111**, 163901 (2017).
[20]F. Cugini, G. Porcari, and M. Solzi, Rev. Sci. Instrum. **85**, 074902 (2014).
[21]J. Döntgen, J. Rudolph, T. Gottschall, O. Gutfleisch, S. Salomon, A. Ludwig, and D. Hägele, Appl. Phys. Lett. **106**, 032408 (2015).
[22]A. P. Kamantsev, V. V. Koledov, A. V. Mashirov, V. G. Shavrov, N. H. Yen, P. T. Than, V. M. Quang, N. H. Dan, A. S. Los, A. Gilewski, I. S. Tereshina, and L. N. Butvin, J. Magn. Magn. Mater. **440**, 70 (2017).
[23]F. Cugini, G. Porcari, C. Viappiani, L. Caron, A. O. dos Santos, L. P. Cardoso, E. C. Passamani, J. R. C. Proveti, S. Gama, E. Bruck, and M. Solzi, Appl. Phys. Lett. **108**(1), 012407 (2016).
[24]F. Cugini, D. Orsi, E. Bruck, and M. Solzi, Appl. Phys. Lett. **113**(23), 232405 (2018).
[25]S. Nikitin, G. Myalikgulyev, A. Tishin, M. Annaorazov, K. Asatryan, and A. Tyurin, Phys. Lett. A **148**, 363 (1990).
[26]A. A. Amirov, A. S. Starkov, I. A. Starkov, A. P. Kamantsev, and V. V. Rodionov, Lett. Mater. **8**(3), 353–357 (2018).
[27]G. Porcari, F. Cugini, S. Fabbrici, C. Pernechele, F. Albertini, M. Buzzi, M. Mangia, and M. Solzi, Phys. Rev. B **86**, 104432 (2012).
[28]G. Porcari, M. Buzzi, F. Cugini, R. Pellicelli, C. Pernechele, L. Caron, E. Brück, and M. Solzi, Rev. Sci. Instrum. **84**, 073907 (2013).
[29]F. Cugini and M. Solzi, J. Appl. Phys. **127**, 123901 (2020).
[30]A. V. Kartasheva, I. N. Flerov, N. V. Volkov, and K. A. Sablina, J. Magn. Magn. Mater. **322**, 622–627 (2010).
[31]L. J. Swartzendruber, Bull. Alloy Phase Diagrams **5**(5), 456–462 (1984).

[32]A. Chirkova, F. Bittner, K. Nenkov, N. V. Baranov, L. Schultz, K. Nielsch, and T. G. Woodcock, Acta Mater. **131**, 31 (2017).
[33]F. Cugini, G. Porcari, S. Fabbrici, F. Albertini, and M. Solzi, Phil. Trans. R. Soc. A **374**, 20150306 (2016).
[34]E. Stern-Taulats, A. Gràcia-Condal, A. Planes, P. Lloveras, M. Barrio, J. L. Tamarit, S. Paramanick, S. Majumdar, and L. Mañosa, Appl. Phys. Lett. **107**, 152409 (2015).
[35]E. Stern-Taulats, T. Castan, A. Planes, L. H. Lewis, R. Barua, S. Pramanick, S. Majumdar, and L. Manosa, Phys. Rev. B **95**, 104424 (2017).
[36]S. O. Mariager, F. Pressacco, G. Ingold, A. Caviezel, E. Mohr-Vorobeva, P. Beaud, S. L. Johnson, C. J. Milne, E. Mancini, S. Moyerman, E. E. Fullerton, R. Feidenhans'l, C. H. Back, and C. Quitmann, Phys. Rev. Lett. **108**, 087201 (2012).